Environ. Sci. Technol. **2010,** *44,* 8601–8608

Application of Raman Microscopy for Simultaneous and Quantitative Evaluation of Multiple Intracellular Polymers Dynamics Functionally Relevant to Enhanced Biological Phosphorus Removal Processes

NEHREEN MAJED AND APRIL Z. GU*

Department of Civil and Environmental Engineering, Northeastern University, 360 Huntington Avenue, Boston, Massachusetts 02115

Received May 14, 2010. Revised manuscript received August 8, 2010. Accepted September 9, 2010.

Polyphosphate (poly-P), polyhydroxyalkanoates (PHAs), and glycogen are the key functionally relevant intracellular polymers involved in the enhanced biological phosphorus removal (EBPR) process. Further understanding of the mechanisms of EBPR has been hampered by the lack of cellular level quantification tools to accurately measure the dynamics of these polymers during the EBPR process. In this study, we developed a novel Raman microscopy method for simultaneous identification and quantification of poly-P, PHB, and glycogen abundance in each individual cell and their distribution among the populations in EBPR. Validation of the method was demonstrated via a batch phosphorus uptake and release test, in which the total intracellular polymers abundance determined via Raman approach correlated well with those measured via conventional bulk chemical analysis (correlation coefficient $r = 0.8$ for poly-P, $r = 0.94$ for PHB, and $r = 0.7$ for glycogen). Raman results, for the first time, clearly showed the distributions of microbial cells containing different abundance levels of the three intracellular polymers under the same environmental conditions (at a given time point), indicating population heterogeneity exists. The results revealed the intracellular distribution and dynamics of the functionally relevant polymers in different metabolic stages of the EBPR process and elucidated the association of cellular metabolic state with the fate of these polymers during various substrates availability conditions.

Introduction

The enhanced biological phosphorus removal (EBPR) process, which employs biological agents (e.g., polyphosphate accumulating organisms (PAOs)) to remove phosphorus (P) from wastewater, is widely applied for achieving low effluent P levels to avoid eutrophication in aquatic water systems. Key biochemical mechanisms involved in the EBPR process include anaerobic uptake and reduction of volatile fatty acid (VFA) into polyhydroxyalkanoates (PHAs, either as poly-β-hydroxybutyrate (PHB) or as polyhydroxyvalerate (PHV)) storage using the energy generated from the hydrolysis of intracellular polyphosphate (poly-P) and the reducing equivalent from glycogen (*1*). In the subsequent aerobic or anoxic phase, PAOs use their stored PHAs as the energy source to support biomass growth, recover cellular glycogen, and restore poly-P accompanied by phosphate uptake. Net P removal from the wastewater is then achieved via the wasting of biomass containing high P content. Another population group that has been found to be relevant and have impact on EBPR process performance is known as glycogen accumulating organisms or GAOs (*2*). Similar to PAOs, GAOs can uptake VFAs in anaerobic condition for PHA formation while using glycogen as the primary source of energy rather than poly-P cleavage like PAOs. GAOs can also oxidize PHAs aerobically leading to biomass growth and glycogen replenishment as PAOs. Since GAOs compete with PAOs for VFAs without contributing to P removal, their presence may impact EBPR systems (*3, 13*). Thus, intracellular storage polymers, such as poly-P, PHAs, and glycogen, play vital roles in the EBPR metabolic dynamics.

Current studies on EBPR process mostly rely on aggregated evaluation of mixed enrichment cultures since there has been no success in isolating pure cultures of PAOs and GAOs. P removal kinetics and stoichiometric assessments also rely mostly on the bulk measurements of the substrates and polymers for the mixed populations during the EBPR process without any quantification at any specific population or cellular level. Evaluation of potential factors that affect the metabolic state, and therefore the abundance and distribution of intracellular polymers, has been very difficult, if not impossible, due to the lack of analytical methods that allow for cellular level quantification of these important storage polymers. Furthermore, quantification of functionally relevant microorganisms, including PAOs and GAOs, have so far been based upon evaluation through molecular tools such as fluorescence in situ hybridization (FISH) or quantitative-polymerase chain reaction (q-PCR) (*4*). Application of these genetic-based molecular techniques, however, is only limited to *in situ* observation and quantification of known PAOs/GAOs, for which the genetic information has been retrieved (*5, 6*). A number of studies have already indicated that the diversity of PAOs and GAOs is larger than currently understood, especially in full-scale EBPR processes (*7, 8, 13*). Therefore, an alternative method to monitor the intracellular storage polymers and their association with metabolic states of diverse groups of PAOs and GAOs populations will greatly improve our understanding of the EBPR fundamentals.

Recently, we have demonstrated successful application of Raman microscopic method for cellular-level quantification and evaluation of intracellular poly-P dynamics in microbial populations during EBPR process (*9*). In this study, we further developed a Raman microscopic method for simultaneous identification and quantification of two other functionally relevant intracellular polymers, namely PHB and glycogen, in microbial cells during EBPR process. The method was, for the first time, applied to evaluate the intracellular distribution and dynamics of the functionally relevant polymers in different metabolic stages of the EBPR process and to elucidate the association of bacterial metabolic state with the fate of these polymers under various substrates availability conditions. Metabolic state-based quantitative identification of PAOs and GAOs populations in the EBPR system based on their intracellular polymers Raman spectrum was proposed.

Materials and Methods

Lab-Scale EBPR System Studied. A laboratory-scale continuous flow EBPR system was established to evaluate P removal performance and to enrich for PAOs and GAOs that

* Corresponding author e-mail: april@coe.neu.edu.

10.1021/es1016526
Published on Web 10/15/2010

could be used for the analysis of intracellular inclusion of poly-P, PHB, and glycogen. The reactor included an anaerobic zone and an anoxic zone, followed by two-stage aerobic zones; the configuration allowed for both A2O (anaerobic−anoxic−oxic) and UCT (University of Cape Town) modes of operation. The HRT and SRT of the system were maintained at 18 h and 8 days, respectively. The composition of synthetic wastewater feed was according to Schuler and Jenkins (*10*). Phosphorus was added as 35.6 mg/L sodium phosphate monobasic ($NaH_2PO_4 \cdot H_2O$) (8 mg P/L). The organic portion of the feeding consisted of 744 mg/L sodium acetate ($CH_3COONa \cdot 3H_2O$) (350 mg COD/L) and 15 mg/L of casamino acids.

Presence of PAOs in the reactor was confirmed with phosphate removal performance evaluation, Neisser staining, and FISH technique. Details on staining and FISH quantification on PAO/GAO abundance and information on the related probes can be found elsewhere (*11*). The FISH probes used for PAO identification were according to Crocetti et al. (*5*) and those for GAOs were according to Crocetti et al. (*6*) and Kong et al. (*12*). The identifiable PAOs/GAOs cells in the reactor seemed to have signature grape-like cocci morphology and they were relatively large (3−5 μm) in comparison to other bacterial cells.

Raman Data Acquisition. Raman spectra were acquired using a WITec, Inc. (Ulm, Germany) model CRM 2000 confocal Raman microscope. Excitation (ca. 30 mW at 633 nm) was provided by a helium/neon laser (Melles Griot, Carlsbad, CA). Details on the acquisition of spectra can be obtained in Majed et al. (*9*). Relative quantity of poly-P content in each individual cell was evaluated based on the Raman intensity (peak height in the unit of charged coupled device (CCD counts) of the PO_2^- stretching band occurring around 1168−1175 cm^{-1} wavenumber region after background correction. The C═O stretching band of ester linkage occurring around 1734 cm^{-1} and glycogen vibration occurring around 480 cm^{-1} were used for quantification of PHB and glycogen content, respectively (see details in Results and Discussion section).

Raman Spectrum with Standard Polymers. Raman spectra of phosphate standards were collected as described in Majed et al. (*9*). Raman spectra for PHB standard were evaluated and identified using commercial chemical poly[(*R*)-3-hydroxybutyric acid] $[COCH_2CH(CH_3)O]_n$. No pure PHV standard is commercially available and a mixture standard that contains 12% PHV by weight mixed with PHB was used for identifying the Raman spectra for PHB in addition to PHV, which was poly(3-hydroxybutyric acid-*co*-3-hydroxyvaleric acid), $[COCH_2CH(CH_3)O]_x[COCH_2CH(C_2H_5)O]_y$. Raman spectra for glycogen were determined with pure glycogen $(C_6H_{10}O_5)_n$. All the chemicals specified above for standardization purposes were obtained from Sigma Chemical Company (St. Louis, MO).

Correlating Intracellular Polymers Quantified by Raman with Those by Bulk Chemical Analysis. To study the dynamics of inclusion of polymers in the cells, P release and uptake tests were performed to allow for obtaining the correlation between the bulk measurements of polymers and the intracellular Raman quantifications. Details of P release and uptake tests can be found in Gu et al. (*13*). For this particular study, the batch testing consisted of 90 min of anaerobic phase with acetate addition (50 mg acetate/L) followed by 240 min of aerobic phase. Samples were taken throughout the P release and uptake tests at 15−90 min intervals. Each sample (10−15 mL) was subjected to both Raman analysis and bulk chemical analysis for the three polymers. The samples, filtered through 0.45-μm filter papers, were analyzed for orthophosphate (ortho-P; $(PO_4^3)^-$) and acetate (CH_3COO^-) using a DX-120 ion chromatograph (Dionex Benelux, Belgium). PHB was measured according to

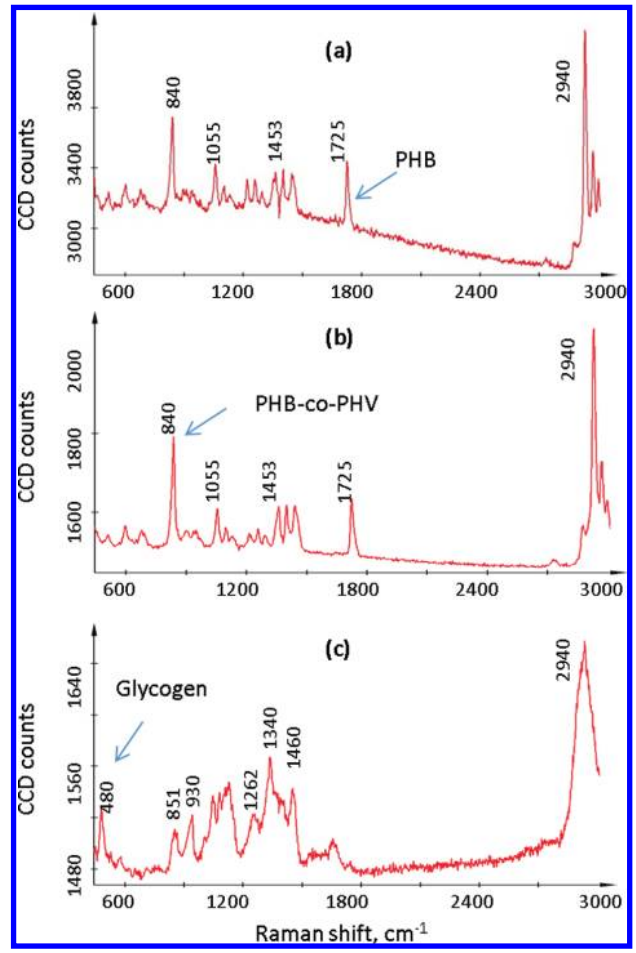

FIGURE 1. Signature Raman spectra of (a) PHB, (b) PHB-co-PHV, and (c) glycogen. Arrows indicate the specific peaks that were selected for quantification of the respective polymers.

the method described in Oehmen et al (*14*). A 3% acidified methanol solution was used for digestion and benzoic acid was used as an internal standard. Standard solutions of PHB were prepared using commercially available poly[(*R*)-3-hydroxybutyric acid] $[COCH_2CH(CH_3)O]_n$ obtained from Sigma Chemical Co.. Samples and standards were digested for 4 h and then extracted according to the method specified. Analysis was performed using a Varian 431 gas chromatograph (Varian, Inc., Palo Alto, CA). Particulate poly-P was analyzed as the difference between the total acid hydrolyzed P and total reactive P and measured according to the standard method (4500-P) (*15*). Glycogen was measured according to the method specified by Erdal (*16*).

Samples subjected to Raman analysis were prepared on optically polished CaF_2 windows (Laser Optex, Beijing, China) according to Majed et al. (*9*). Raman spectra for at least 40−45 single cells were examined for each sample (the sample size required to obtain statistically reliable results was previously determined to be greater than 30 cells per sample) (*9*).

Results and Discussion

Characteristic Raman Spectra of Polymers. Figure 1a shows the Raman spectrum of the commercially available PHB. The most prominent bands in this spectrum are located at 433, 840−860, and 1725−1734 cm^{-1} and can be assigned to δ(CC) skeletal deformations, ν(CC) skeletal stretches, and ν(C═O) stretching vibrations respectively, and these are consistent with the Raman spectra of PHB as examined by Lin-Vien (*17*). The regions from 1040 to 1140 cm^{-1} and from 1250 to 1460 cm^{-1} show bands originated from ν(CC) skeletal stretches and δ(CH), δ(CH2), and δ(CH3) deformations,

respectively (*17*). Figure 1b shows the Raman spectrum of the PHB-co-PHV copolymer (with 12% PHV content) which shows the same bands as those of PHB, except that the relative intensity of skeletal stretches at 840 cm^{-1} for the copolymer is higher with respect to ν(C═O) stretching at 1734 cm^{-1} than that of PHB alone. This is likely due to the additional CH_2 in the alkyl side groups of the PHV. The nature of this predominately skeletal C−C stretching vibration has been shown to be dependent on the number of carbons in *n*-alkanes (*18*). Figure 1c shows the Raman spectrum of pure glycogen, which is similar to the spectra of glycogen reported previously (*19*). It is observed that the glycogen vibrations mainly occur at the peak positions around 478−484, 840−860, 937−944, 1048−1087, 1131, 1333−1383, and 1460 cm^{-1} (*20*−*22*) and these regions correspond to skeletal deformation, CC skeletal stretch, ring "breathing", ring vibration, pseudosymmetric C═*C*═O stretch, CH_3 symmetric deformation, and CH_3, CH_2 deformations, respectively (*17*). Identification and standardization of peak positions for poly-P of different chain lengths have been described previously (*9*), and the signature peaks associated with poly-P are P−O−P vibrations and PO_2^- stretches, with vibrations occurring at around 690 and around 1157 cm^{-1}, respectively.

Simultaneous Observation of Intracellular Polymers in EBPR Process. It is recognized that all Raman-active biomolecules in a cell will contribute to the resulting spectrum and their signals may overlap (*23*). Thus, it is crucial to identify one representative peak of each polymer which is unique and representative of the specific polymer without any or with minimal interference from the others. Raman band positions of the polymers in the reference (standard) spectrum and in the bacterial spectra may differ by several wavenumbers, because of the different physicochemical state of the polymer and a different matrix in bacteria (*23*). We found that the band position around 1734 cm^{-1} representing C═O stretching vibrations of the ester linkage could be the potential marker for PHB (*23*) and the best indicator for glycogen is the glycogen vibration occurring around 480 cm^{-1} peak position (*21*). The intensities of these mentioned peaks were then used to quantify the cellular PHB and glycogen content, respectively. Since there was no commercially available PHV, we used PHB/PHV copolymer for observing signature spectrum for the presence of PHV. We found that PHV presence caused the increased intensity of peak at 840 cm^{-1} and led to a higher ratio (>1) of the intensity of ν(CC) skeletal stretches at 840 cm^{-1} to the vibrations at 1734 cm^{-1} ($intensity_{860\ cm^{-1}}/intensity_{1734\ cm^{-1}}$), which is approximately 1 for spectrum for PHB only. The Raman band of PO_2^{-1} vibrations occurring around 1168−1177 cm^{-1} was considered as the potential indicator and quantifiable peak for poly-P (*9*).

We observed diverse and different combinations of intracellular polymeric inclusions inside individual cells obtained from different anaerobic and aerobic stages of EBPR processes (Figure 2). Eight types of cellular Raman spectra (assuming each represents one metabolic state of a cell) have been identified and they include cells with none of the signature peaks for any of the three polymers, cells with only one of the polymer inclusion, and cells with different combinations of the three polymers, as shown in Figure 2.

Note that for cells that contained both PHB/PHV and glycogen, we found that the overlapping of the 840 cm^{-1} band region from PHB/PHV with the 840−860 cm^{-1} band region from glycogen made it difficult to differentiate the PHB from PHB/PHV coexistence. Thus, PHV cannot be accurately quantified for cells that contain relatively high levels of both PHAs and glycogen. Cells having PHAs without any glycogen inclusion can be evaluated for the presence of both PHB and PHV based on the relative peak intensities of the bands at 840 and 1734 cm^{-1} according to the standards. It has been shown that the PHB or PHV content depends on the substrate type; when fed with acetate, PAOs produce mainly PHB (generally <10% PHV production) (*24, 25*), while GAOs produce approximately 75% PHB and 25% PHV (*26*). Therefore, for our acetate-fed EBPR system, PHB is expected to be the dominant type of PHA. This is also true for most full-scale EBPR processes since VFAs in the wastewater influent are mostly acetate unless supplemented with others (*13, 27*). However, it should be recognized that PHV is the primary PHA fraction produced by GAOs when fed with propionate (*28*). Based on the metabolic pathways and involvement of these polymers in PAOs and GAOs, the spectra as shown in Figure 2 may potentially allow for identification of PAOs and GAOs based on their metabolic state. For example, spectra shown in Figures 2b, e, f, and h likely represent PAO cells and those in 2d and g likely present GAO cells. Endeavors are underway in our lab to further investigate the identification of relevant PAOs and GAOs based on their Raman spectra.

Correlation between the Polymers Abundance Quantified via Raman Microscopy and Those Measured by Chemical Analysis. To validate the intracellular polymer identification and quantification by the Raman microscopy method developed, we simultaneously measured and compared the polymer content in the biomass via both Raman analysis and conventional chemical analysis. Correlation plots of Raman measurements versus chemical analyses for all the polymers are provided in Supporting Information (SFigure 1) and they showed that measurements of the three polymers by the two methods are consistent with determined correlation factors (*r*) of 0.80, 0.94, and 0.70 for poly-P, PHB, and glycogen, respectively. Figure 3a, b, and c show the profiles of poly-P, PHB, and glycogen content determined via both Raman method and bulk chemical measurement, respectively, during the P release and uptake testing time period. Figure 3a shows that the profile of poly-P intensities determined by Raman method correlated well with the ortho-P profile (correlation coefficient, $r = -0.93$) and it correlated with the bulk particulate poly-P profile as well ($r = 0.8$). Acetate was consumed within 30 min of the anaerobic period (data not shown), concomitantly with the P release at a rate of 10.1 mg -P/g VSS·h. Total intracellular poly-P intensity decreased significantly from 3406 to 1709 CCD counts, and so did the bulk poly-P, during the first 30 min of anaerobic period concurring with the phosphate release. The extended anaerobic phase after the complete consumption of acetate represents substrate starvation situation for the PAOs, during which a very low release of P (net release of 0.47 mg P/L from 45 to 90 min) was observed likely attributed to the cell maintenance release (*29*). P uptake occurs in the subsequent aerobic phase at a rate of 4.26 mg P/g VSS·h and reaches zero at the end of the aerobic period. One interesting observation (from multiple experiments) is that at the end of the extended aerobic phase (>300 min time period), intracellular poly-P level (by Raman analysis) started to decline (Figure 3a). Secondary aerobic P release due to poly-P utilization for cell maintenance at depletion of stored PHB during extended aeration has been suggested previously (*26*). However, the reason for why the intracellular poly-P decreases, as indicated by our Raman analysis, did not witness the concurrent increase in the bulk ortho-P concentration in the liquid is puzzling and requires further investigation.

The total Raman intensity profile for PHB correlated well with the bulk PHB measurements via chemical analysis (Figure 3b, SFigure 1b), and they showed continuous cellular replenishment simultaneously with poly-P break down and ortho-P release for the first 60 min of the anaerobic period. The end of the anaerobic phase (60−90 min) witnessed PHB depletion probably due to starvation condition, suggesting that cellular PHB could be consumed under anaerobic

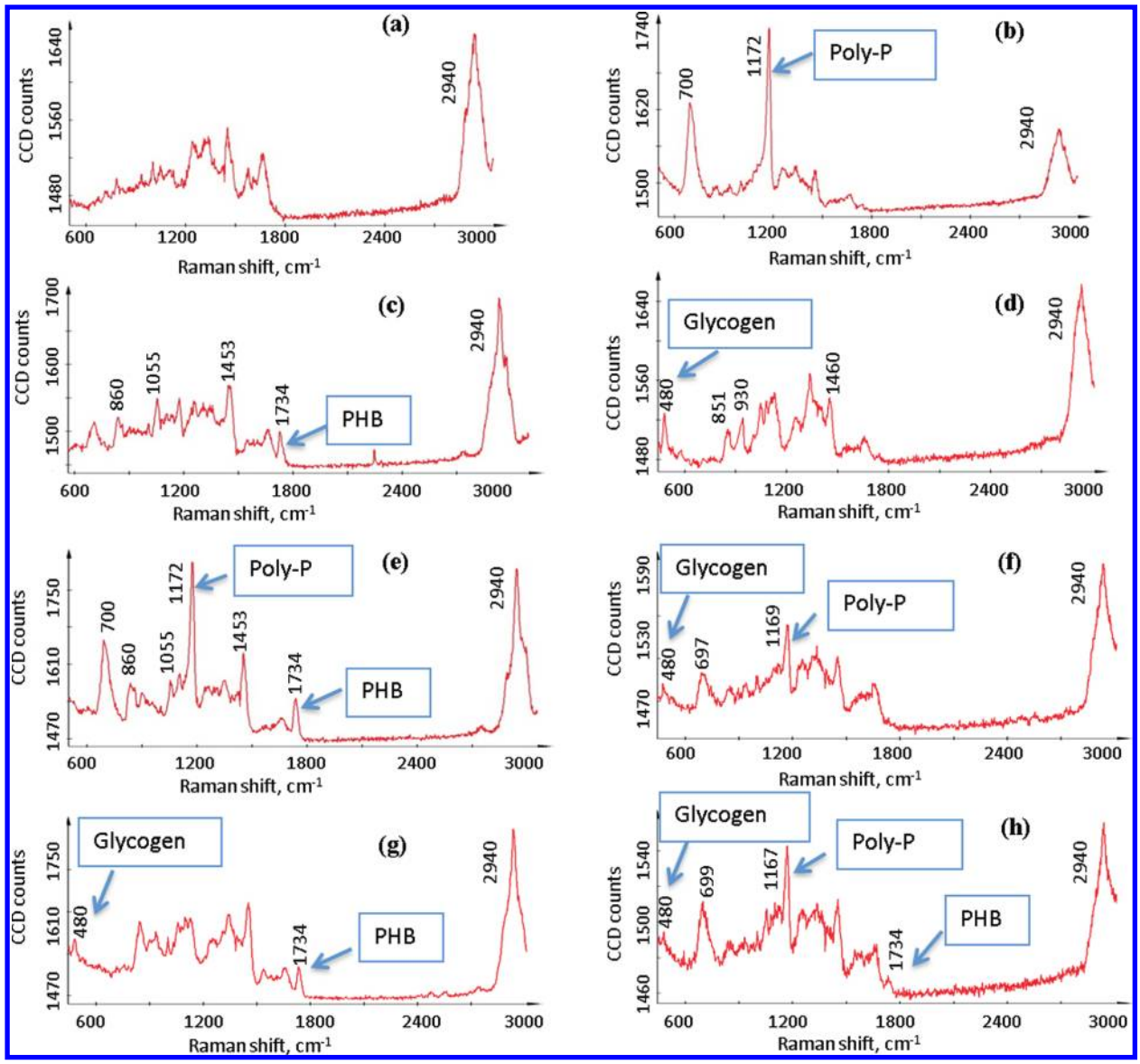

FIGURE 2. Raman spectra of microbial cells that contained different combinations of the three polymers, representing various metabolic states of cells during EBPR process. These include cells containing (a) no polymer; (b) only poly-P; (c) only PHB; (d) only glycogen; (e) poly-P and PHB; (f) poly-P and glycogen; (g) glycogen and PHB; and (h) poly-P, PHB, and glycogen.

conditions upon complete consumption of acetate and when P release almost ceases. PHB utilization continued in the following aerobic phase for 180 min and seemed to reach a plateau when the internal poly-P utilization occurred (as discussed above).

The total glycogen associated with biomass determined by Raman also correlated relatively well with that measured by chemical analysis (Figure 3c, SFigure 1c). With the quick ortho-P release and PHB replenishment in the cells during the initial anaerobic period (<45 min), glycogen content declined as shown by both the Raman glycogen intensity and by the measured glycogen profiles (Figure 3c). During the later anaerobic period, level of glycogen showed slight increment probably due to PHB depletion in the absence of VFAs. Then in the subsequent aerobic period, glycogen recovered rather rapidly until the 250-min time point, and the overall glycogen profiles seemed to plateau until the end of the aerobic period. This seemed to coincide with the depletion of PHB during the extended aeration period as discussed above. Previous studies on EBPR with PAO enriched systems (*4*, *30*) have reported continuous depletion of glycogen in a prolonged anaerobic phase (~120 min) followed by continuous replenishment in the aerobic phase where the level became fairly constant beyond 2 h of aeration. However, an important point to note is that the total glycogen profiles here reflect the combined glycogen content in both PAOs and GAOs. Above results demonstrated and validated that the developed Raman method can successfully quantify the abundances of cellular poly-P, PHB, and glycogen in an EBPR system at both individual and population levels.

Relative Distribution of the Polymers among the Cells. Figure 4 and SFigure 2 show the abundance distribution of cells containing different levels of intracellular poly-P, PHB, and glycogen in the samples taken at different time points during the P uptake and release testing. At any given time point during the EBPR process, there is a distribution of microbial cells containing different abundance levels of intracellular polymers among individual cells even under the same environmental conditions, indicating that heterogeneity exists in the cellular metabolic state and storage products. This heterogeneity could result from either the phylogeny or the biomass division or other kinetic parameters (e.g., P release or acetate uptake rates) (*32*). From all the Raman analyzed cells, the glycogen intensities ranged from 5 to 144 CCD and the PHB intensities ranged from 5 to 110

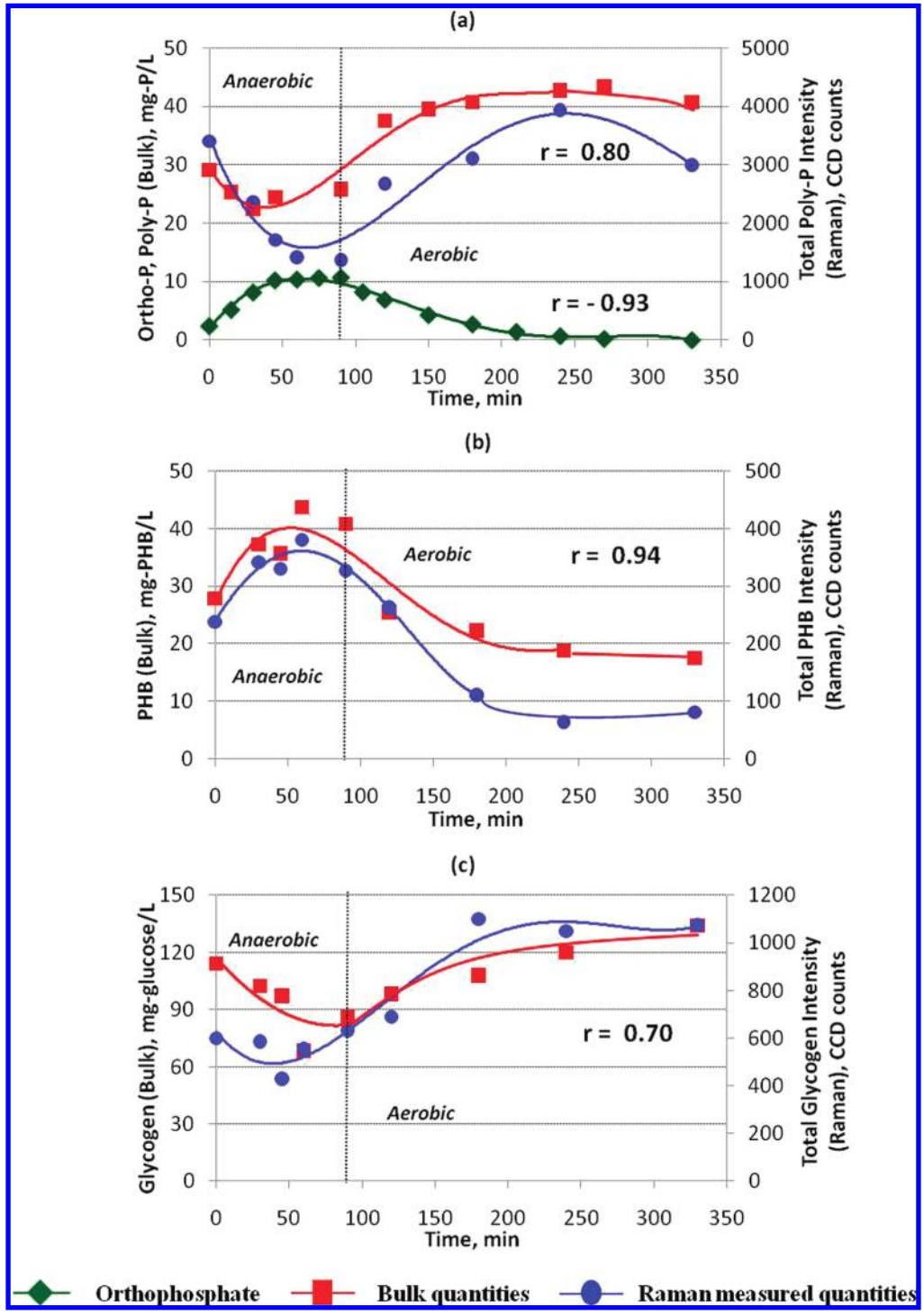

FIGURE 3. Correlation of various intracellular polymer abundance determined by Raman analysis with those measured by chemical analysis during the anaerobic/aerobic P uptake and release batch testing. Correlation of (a) intracellular poly-P measured by Raman analysis with particular poly-P measured by chemical analysis and with soluble ortho-P in solution; (b) PHB measured by Raman analysis with those measured via chemical analysis; (c) glycogen measure by Raman analysis with those measured via chemical analysis. Correlation coefficients are shown in the figures.

CCD, suggesting that there might be a "maximum" saturation level of these polymers in each cell. The "saturation" levels of these polymers affect the metabolic state of cells. Whether these saturation levels vary among different PAOs in various EBPR systems and what factors may affect these saturated polymeric inclusion levels can be further investigated with the Raman microscopy method developed here. These distributions of EBPR storage polymers among microbial cells suggest that an agent-based modeling to capture the heterogeneity among individual biological agents can more accurately reflect the microbial functions in the EBPR system (*31*, *32*).

In general, the distribution and fractions of cells with different levels of polymeric inclusions were consistent and reflective of the specific metabolic stage during the EBPR process. For example, at the initial anaerobic stage, more than 50% of the cells in the culture had poly-P content greater than 30 CCD and this fraction decreased from 50% to 20%

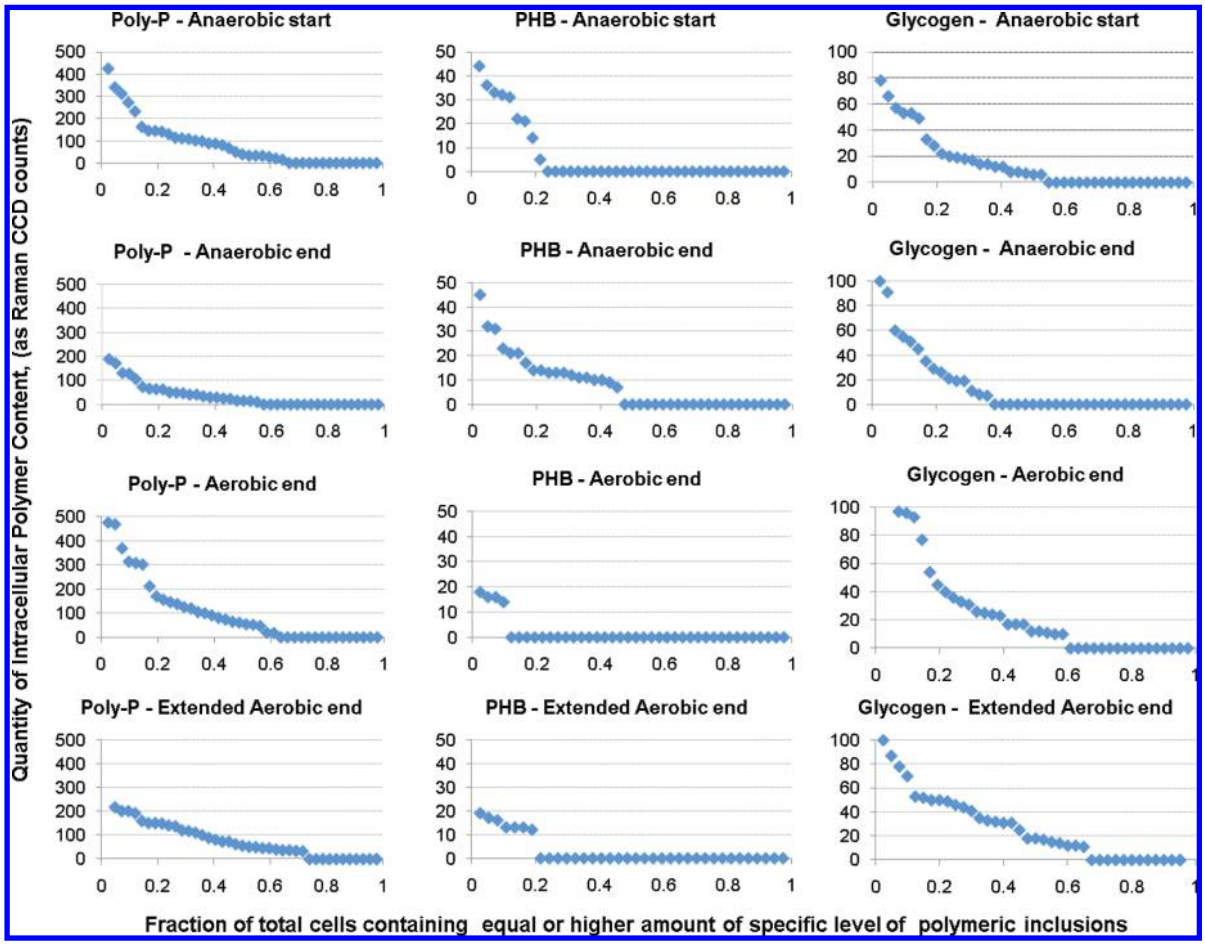

FIGURE 4. Intracellular polymer abundance (intensity) distribution among population cells for polyphosphate, PHB, and glycogen quantities (as CCD counts), repectively, at various time points of anaerobic and aerobic phases during the phosphate release and uptake test: anaerobic start = 0 min; anaerobic end = 90 min; aerobic end = 240 min; and extended aerobic end = 330 min. *X* axis: fractions of cells that contained equal or higher amount of the specific level of polymeric inclusion at any given time point.

at the end of the anaerobic phase as poly-P being utilized and released as ortho-P. The maximum level of intracellular poly-P content decreased from >400 to <200 CCD. The subsequent aerobic P uptake phase led to the overall increase in the poly-P content in the population, with more than 58% of the cells containing poly-P higher than 30 CCD. An interesting observation is that with the extended aeration period (>330 min), overall abundance of poly-P seemed to decline again, as indicated by decrease in both the highest level of poly-P observed and fractions of cells containing higher level (>50 CCD) of poly-P. A possible explanation for this observation related to aerobic secondary release of P was discussed earlier.

For intracellular distribution of PHB, only 20% of the population had detectable PHB inclusion (>0 CCD counts) at the beginning of the anaerobic phase, and it increased to 45% at the end of the anaerobic uptake of acetate and PHB formation. The following aerobic phase led to consumption of PHBs and corresponding decease in the percentage of cells containing PHB to 11%. Interestingly, with extended aeration, there seemed to be a slight increase in the fraction of cells containing PHB inclusion, which is not clearly understood. Distribution of cells with various levels of glycogen also showed corresponding shifts as the population underwent the anaerobic and aerobic cycles during the EBPR process. The fraction of cells containing glycogen >10 CCD counts decreased from 40% to 30% from the beginning to the end of the anaerobic phase, and then again increased to 60% at the end of the aerobic phase. Extended aeration seemed to lead to a slight increase in the percentage of cells possessing glycogen polymer as well.

The total population level and distribution of cells containing different levels of glycogen and PHB is more complicated compared to poly-P, because both PHB and glycogen play roles in metabolic pathways for both PAOs and GAOs. Since our reactor contained both PAOs and GAOs (based on FISH results and the $P_{release}/HAc_{uptake}$ ratio of 0.30 P-mol/C-mol which also suggests coexistence of PAOs/GAOs (*13*)), the cellular glycogen distribution during the EBPR process is the combination effect of both PAOs and GAOs. Because of the involvement of glycogen in both PAOs and GAOs metabolism, separate characterization of intracellular glycogen content between PAOs and GAOs will be useful to understand the overall glycogen abundance trend and distribution among the two groups of population, which warrants further investigation.

Implications of Intracellular Polymers Quantification in EBPR. Cellular storage products play key roles in the basic EBPR mechanism and therefore the ability to quantify their abundance dynamics at cellular level is crucial for fundamental understanding of the EBPR process. Currently, EBPR studies are mostly conducted with enriched mixed culture due to the absence of availability of isolates. Usually, bulk measurements representing the overall average state of the EBPR sludge matrix pertaining to a particular condition and at a given time point are applied to determine the kinetics and stoichiometry of the process. However, the combined effect of mixed populations in the

system on the kinetics data often makes the interpretation difficult. Investigation of the EBPR mechanisms at the population level, especially at full-scale EBPR systems, has been limited so far because of the inability of the available molecular techniques to capture PAOs and GAOs beyond those identified from lab-scale, often acetate-fed systems. In addition, it is often difficult to associate the genotype identification with phenotype state, considering that phylogenetic characterization does not always correlate with the metabolic states of microorganisms. For example, PAOs quantified by FISH do not necessarily reflect the active population that contributes to EBPR. Advanced techniques such as FISH combined with microautoradiography are useful to identify and understand the in vivo physiology, diversity, and activity of functional microbial groups in biological processes (*33*), but those are also restrained by the FISH probes available. Intracellular identification and quantification of poly-P, PHB, and glycogen polymers, as shown in this study, allowed for the observation of distributed states of storage polymers at cellular level in functionally relevant microbial populations pertaining to EBPR under different environmental conditions. This would allow further study to gain more fundamental understanding of the metabolic pathways involving the various polymers, as well as the process kinetics relating to the EBPR performance. Furthermore, our preliminary results suggest that simultaneous identification of all three intracellular polymers in each individual cell may potentially enable us to identify PAO and GAO cells based on their unique polymers' Raman spectrum and consequently their metabolic state. This will ultimately provide us with the opportunity to differentiate the levels of polymeric inclusions in different populations, which is not possible currently by relying on bulk chemical analysis only. Because most full-scale EBPR processes have mixed populations of PAOs and GAOs (*11, 12, 13*) and their relative abundance and related activities impact the stability and efficiency of EBPR process, it is crucial to be able to monitor the population dynamics and associated functions and performance for diverse populations beyond those identifiable by available genetic markers only. This study demonstrated the potential application of Raman microscopy to quantitatively investigate the dynamics of the functionally relevant polymers linked with population metabolic state, which can elucidate the behavior of an EBPR system at a much more detailed and fundamental level.

Acknowledgments

This study was funded by scholarship to ITRI-NU (Industrial Translational Research Initiative at NU) from R&D of AnoxKaldnes Inc. Sweden (Now Veolia Water Solutions and Technologies). We greatly thank Professor Max Diem and Dr. Christian Matthäus in the department of Chemistry and Chemical Biology at Northeastern University for their advice and assistance in Raman microscopic analysis. We also acknowledge Professor John D. Savage in the Department of Science at Middlesex Community College for his valuable guidance with Raman spectrum analysis and principles.

Supporting Information Available

Two additional figures for clarification: SFigure 1, showing the correlation plots of various intracellular polymer abundance determined by Raman analysis versus those measured by chemical analysis during the anaerobic/aerobic P uptake and release batch testing; and SFigure 2, showing the bar graph of abundance distribution of cells with different levels of intracellular polyphosphate, PHB, and glycogen quantities at various time points of anaerobic and aerobic phases during the phosphate release and uptake test. This material is available free of charge via the Internet at http://pubs.acs.org.

Literature Cited

(1) Mino, T.; Arun, V.; Tsuzuki, Y.; Matsuo, T. Effect of phosphorus accumulation on acetate metabolism in the biological phosphorus removal. In *Biological Phosphate Removal from Wastewaters*; Ramadori, R., Ed.; Advances in Water Pollution Control Series, vol. 4; 1987; pp 27−38.

(2) Liu, W. T.; Mino, T.; Nakamura, K.; Matsuo, T. Glycogen accumulating population and its anaerobic substrate uptake in anaerobic-aerobic activated sludge without biological phosphorus removal. *Water Res.* **1996**, *30* (1), 75–82.

(3) Satoh, H.; Mino, T.; Matsuo, T. Deterioration of enhanced biological phosphorus removal by the domination of microorganisms without polyphosphate accumulation. *Water Sci. Technol.* **1994**, *30* (6), 203–211.

(4) Bond, P. L.; Erhart, R.; Wagner, M.; Keller, J.; Blackall, L. L. Identification of some of the major groups of bacteria in efficient and nonefficient biological phosphorus removal activated sludge systems. *Appl. Environ. Microbiol.* **1999**, *65* (9), 4077–4084.

(5) Crocetti, G. R.; Hugenholtz, P.; Bond, P. L.; Schuler, A.; Keller, J.; Jenkins, D.; Blackall, L. L. Identification of polyphosphate-accumulating organisms and design of 16S rRNA-directed probes for their detection and quantitation. *Appl. Environ. Microbiol.* **2000**, *66* (3), 1175–1182.

(6) Crocetti, G. R.; Banfield, J. F.; Keller, J.; Bond, P. L.; Blackall, L. L. Glycogen-accumulating organisms in laboratory-scale and full-scale wastewater treatment processes. *Microbiology* **2002**, *148*, 3353–3364.

(7) Gu, A. Z.; Saunders, A. M.; Neethling, J. B.; Stensel, H. D.; Blackall, L. *Investigation of PAOs and GAOs and their effects on EBPR performance at full-scale wastewater treatment plants in US*. In Proceedings, WEFTEC 05, Washington, DC, 2005.

(8) Wong, M. T.; Mino, T.; Seviour, R. J.; Onuki, M.; Liu, W. T. In situ identification and characterization of the microbial community structure of full-scale enhanced biological phosphorous removal plants in Japan. *Water Res.* **2005**, *39* (13), 2901–2914.

(9) Majed, N.; Matthaus, C.; Diem, M.; Gu, A. Z. Evaluation of intracellular polyphosphate dynamics in enhanced biological phosphorus removal process using Raman microscopy. *Environ. Sci. Technol.* **2009**, *43* (11), 5436–5442.

(10) Schuler, A. J.; Jenkins, D. Enhanced biological phosphorus removal from wastewater by biomass with different phosphorus contents, part I: Experimental results and comparison with metabolic models. *Water Environ. Res.* **2003**, *75* (6), 485–498.

(11) Majed, N., Onnis-Hayden, A., Christensson, M., Welander, T. Gu, A. Z. In *Phosphorous Removal Kinetics and Operational Issues with a Lab-Scale Advanced IFAS-EBPR-MBR Process*. In Proceedings, WEFTEC08, Chicago, IL, 2008.

(12) Kong, Y. H.; Ong, S. L.; Ng, W. J.; Liu, W. T. Diversity and distribution of a deeply branched novel proteobacterial group found in anaerobic-aerobic activated sludge processes. *Environ. Microbiol.* **2002**, *4* (11), 753–757.

(13) Gu, A. Z.; Saunders, A.; Neethling, J. B.; Stensel, H. D.; Blackall, L. L. Functionally Relevant Microorganisms to Enhanced Biological Phosphorus Removal Performance at Full-Scale Wastewater Treatment Plants in the United States. *Water Environ. Res.* **2008**, *80* (8), 688–698.

(14) Oehmen, A.; Keller-Lehmann, B.; Zeng, R. J.; Yuan, Z. G.; Keller, E. Optimisation of poly-beta-hydroxyalkanoate analysis using gas chromatography for enhanced biological phosphorus removal systems. *J. Chromatogr. A* **2005**, *1070* (1−2), 131–136.

(15) APHA. *Standard Methods for the Examination of Water and Wastewater*, 20th ed.; American Public Health Association: Washington, DC, 1998.

(16) Erdal, Z. K. The Biochemistry of EBPR: Role of Glycogen in Biological Phosphorus Removal and the Impact of the Operating Conditions on the Involvement of Glycogen. PhD Dissertation, Virginia Tech, Blacksburg, VA, 2002.

(17) Lin-Vien, D., Colthup, N. B., Fateley, W. G., Grasselli, J. G. *The Handbook of Infrared and Raman Characteristic Frequencies of Organic Molecules*; Academic Press: San Diego, CA, 1991.

(18) Dollish, F. R.; Fateley, W. G.; Bentley, F. F. *Characteristic Raman Frequencies of Organic Compounds*; John Wiley & Sons: New York, 1974.

(19) Choo-Smith, L. P.; Maquelin, K.; van Vreeswijk, T.; Bruining, H. A.; Puppels, G. J.; Thi, N. A. G.; Kirschner, C.; Naumann, D.; Ami, D.; Villa, A. M.; Orsini, F.; Doglia, S. M.; Lamfarraj, H.; Sockalingum, G. D.; Manfait, M.; Allouch, P.; Endtz, H. P. Investigating microbial (micro)colony heterogeneity by vibra-

tional spectroscopy. *Appl. Environ. Microbiol.* **2001**, *67* (4), 1461–1469.
(20) Shetty, G.; Kendall, C.; Shepherd, N.; Stone, N.; Barr, H. Raman Spectroscopy: Elucidation of Biochemical Changes in Carcinogenesis of Oesphagus. *Br. J. Cancer* **2006**, *94*, 1460–1464.
(21) Castillo, C. G.; Lo, W. K.; Kuck, J. F. R.; Yu, N. T. Nature and localization of avian lens glycogen by electron microscopy and Raman spectroscopy. *Biophys. J.* **1992**, *61* (4), 839–844.
(22) Stone, N.; Kendall, C.; Smith, J.; Crow, P.; Barr, H. Raman Spectroscopy for Identification of Epithelial Cancers. *Faraday Discuss.* **2004**, *126*, 141–157.
(23) De Gelder, J.; Willemse-Erix, D.; Scholtes, M. J.; Sanchez, J. I.; Maquelin, K.; Vandenabeele, P.; De Boever, P.; Puppels, G. J.; Moens, L.; De Vos, P. Monitoring poly(3-hydroxybutyrate) production in Cupriavidus necator DSM 428 (H 16) with Raman spectroscopy. *Anal. Chem.* **2008**, *80* (6), 2155–2160.
(24) Mino, T.; Van Loosdrecht, M. C. M.; Heijnen, J. J. Microbiology and biochemistry of the enhanced biological phosphate removal process. *Water Res.* **1998**, *32* (11), 3193–3207.
(25) Satoh, H, M. T.; Matsuo, T. Uptake of organic substrates and accumulation of polyhydroxyalcanoates linked with glycolysis of intracellular carbohydrates under anaerobic conditions in the biological excess phosphate removal processes. *Water Sci. Technol.* **1992**, *26* (5−6), 933–942.
(26) Filipe, C. D. M.; Daigger, G. T.; Grady, C. P. L. A metabolic model for acetate uptake under anaerobic conditions by glycogen accumulating organisms: Stoichiometry, kinetics, and the effect of pH. *Biotechnol. Bioeng.* **2001**, *76* (1), 17–31.
(27) Neethling, J. B.; Bakke, B.; Benisch, M.; Gu, A. Z.; Stephens, S.; Stensel, H. D. *Factors Influencing the Reliability of Enhanced Biological Phosphorus Removal*; Report 01-CTS-3; Water Environment Research Foundation: Alexandria, VA, 2005.
(28) Oehmen, A.; Zeng, R. J.; Yuan, Z. G.; Keller, J. Anaerobic metabolism of propionate by polyphosphate-accumulating organisms in enhanced biological phosphorus removal systems. *Biotechnol. Bioeng.* **2005**, *91* (1), 43–53.
(29) Pijuan, M.; Saunders, A. M.; Guisasola, A.; Baeza, J. A.; Casas, C.; Blackall, L. L. Enhanced biological phosphorus removal in a sequencing batch reactor using propionate as the sole carbon source. *Biotechnol. Bioeng.* **2004**, *85* (1), 56–67.
(30) Lu, H.; Oehmen, A.; Virdis, B.; Keller, J.; Yuan, Z. Obtaining highly enriched cultures of Candidatus Accumulibacter phosphates through alternating carbon sources. *Water Res.* **2006**, *40*, 3838–3848.
(31) Schuler, A. J. Diversity matters: Dynamic simulation of distributed bacterial states in suspended growth biological wastewater treatment systems. *Biotechnol. Bioeng.* **2005**, *91* (1), 62–74.
(32) Schuler, A.; Majed, N.; Bucci, V.; Hellweger, F. L.; Tu, Y.; Gu, A. Z. Is the whole the sum of its parts? Agent-based modelling of wastewater treatment systems. *Water Sci. Technol.* **2010**, (Accepted).
(33) Nielsen, P. H.; Andreasen, K.; Lee, N.; Wagner, M. Use of microautoradiography and fluorescent in situ hybridization for characterization of microbial activity in activated sludge. *Water Sci. Technol.* **1999**, *39* (1), 1–9.

ES1016526